RSC Advances

ROYAL SOCIETY OF CHEMISTRY

www.rsc.org/advances

Cite this: DOI: 10.1039/c0xx00000x

www.rsc.org/xxxxxx

ARTICLE TYPE

Glutathione-directed synthesis of luminescent Ag_2S nanoclusters as nanosensors for copper(II) ion and temperature

Lingcan Kong,*[a] Wenwei Liu,[a] Xuefeng Chu,[b] Yuyang Yao,[a] Pengfei Zhu[a] and Xia Ling*[a]

Received (in XXX, XXX) Xth XXXXXXXXX 20XX, Accepted Xth XXXXXXXXX 20XX

DOI: 10.1039/b000000x

Highly red luminescent and water-soluble Ag_2S nanoclusters (NCs) are synthesized using glutathione as a stabilizing and capping agent. The as-prepared NCs have been characterized in terms of photoluminescence excitation spectrum, photoluminescence spectrum, transmission electron microscopy, fourier transform infrared spectroscopy, and X-ray photoelectron spectroscopy. The NCs are shown to be viable fluorescent probes for the determination of Cu^{2+} ion due to aggregation-induced quenching of fluorescence. Furthermore, the nanosensor exhibits high sensitivity to Cu^{2+} ion with a detection limit of 2.5 nmol·L^{-1} and has been demonstrated for determination of Cu^{2+} ion in real water samples including tap water, mineral water, and Taihu lake water. In addition, the as-prepared NCs could be used as versatile nanothermometry devices in cellular and in vivo temperature sensing based on obvious temperature dependence on the logarithm of fluorescence emission intensity, which changes obviously over physiological temperature range (6–50°C).

Introduction

The determination of metal ions in the environment is of particular interest owing to their beneficial and/or hazardous effects on human health.[1] Copper is a kind of heavy metal element which plays an important role in cooperating with some proteins to produce numerous enzymes critical for life.[2] However, copper ions are toxic when its level exceeds cellular needs, which will cause serious diseases, such as Alzheimer's disease, Menkes disease, and Wilson disease.[3] Due to the widespread use of copper compounds in agriculture and industry together with its difficulty in biological detoxification, copper contamination and its potential toxicity on human being are challenging problems throughout the world.[4] Currently, several analytical methods have been employed for copper determination, such as atomic absorption spectrometry (AAS),[5] inductively coupled plasma atomic emission spectrometry (ICP-AES),[6] inductively coupled plasma mass spectrometry (ICP-MS).[7] These methods often require expensive, complicated instrumentation and time-consuming, which hampers their practical application for in-field measurement.[8] It is of considerable significance to develop highly sensitive and selective probes for copper determination.

On the other hand, temperature plays an important role in biochemistry and physiological processes.[9] The accurate measure of it is of tremendous significance owing to its widespread use in medical diagnostics and electronic devices.[10] Thus far, some promising materials have been employed to measure temperature in terms of fluorescence spectra or Raman spectroscopy.[11,12] Among them, fluorescence-based materials are of increasing interest due to their high resolution and fast responses.[13] Indeed, several fluorescent nanomaterials including organic dyes, semiconductor quantum dots have been employed for temperature detection, which operates by temperature-dependence emission intensity changes.[14] Furthermore, fluorescence metal nanoclusters have already shown great potential for temperature sensor in biological systems and live cells.[15] However, the complicate synthesis, toxicity, or expensive price make some materials unsuitable for many practical application. Thus from the viewpoint of practical applications, an excellent probe should be not only highly sensitive and selective but also simple, safe, and economical simultaneously.

Metal clusters are interesting classes of materials that are known to be isolated particles with several to a hundred atoms smaller than 10 nm in size.[16] Due to their molecular-like electronic transitions and strong fluorescence, nanoclusters (NCs) materials has been extensively studied for potential applications in nanodevices, biological labeling, novel catalysis, ion sensing, and various other applications.[17–19] Similar to quantum dots, metal NCs show size-dependence tunable fluorescence from visible to near infrared regions with high quantum yields.[20] Biomolecule-conjugated fluorescent metal NCs have been considered as a powerful technique for the detection of low concentration analytes due to their facile synthesis, low cost, environmental benign, and multifunctional surface chemistry.[21] For example, Lin and coworkers reported Ag NCs for highly selective detection of Hg^{2+} ion at ppb level.[22] Wang and coworkers used red fluorescent nanoclusters as effective probe for Cu^{2+} ion.[23] Although there are a number of reports on the detection of low concentration analytes by using fluorescent NCs,[24] corresponding studies on metal NCs thermometers are very rare.[25]

Recently, metal nanoclusters have been successfully applied in fluorescent detection of metal ions, small molecules, protein, DNA and miRNA as well as biological labeling and imaging.[26] For example, Chen and coworkers demonstrated glutathione-capped gold nanoclusters were capable of sensing Cu^{2+} ion.[27] Santhosh and coworkers developed human serum albumin stabilized metal nanoclusters, which could be applied for the detection of free bilirubin in blood serum as fluorometric and colorimetric probe.[28] Jiang and coworkers have developed a colorimetric detection system for glucose based on the peroxidase-like activity of apoferritin paired metal clusters.[29]

However, to the best of our knowledge, the detection of copper ion via Ag_2S nanoclusters has been rare. On the other hand, nanoscale thermal probe by metal nanoclusters was also rarely reported.[30] Herein, we proposed a novel fluorescent sensor showing highly sensitivity and selectivity detection of copper ion and temperature based on glutathione protected Ag_2S nanoclusters. It is envisaged that the combination of strong fluorescent properties of Ag_2S NCs and water-soluble as well as biocompatible characters of glutathione moiety together with the detection of low concentration metal ions and nanothermometry devices over the physiological temperature range may provide attractive multifunctional features for the development of multifunctional materials. This will allow the systematic study of the influence of metal ions/temperature on Ag_2S NCs protected by glutathione, which will provide important insights into the future design of multifunctional materials. Herein are described the design and synthesis of Ag_2S NCs with red emission. As-prepared NCs are protected by glutathione which could work as an important capping agent to prevent NCs from becoming large nanoparticles.[31] More importantly, many functional groups including thiols, carboxyl, and amino groups make fluorescent NCs exhibit good dispersion and high stability in water.[32] These advantages suggest that the resultant Ag_2S NCs are promising fluorescent probes for detection of heavy-metal ions and cellular temperature sensing in aqueous solution.

Experimental

Materials

Reduced glutathione (GSH, molecular weight of 307 $g \cdot mol^{-1}$) was purchased from Aldrich. Silver nitrate ($AgNO_3$, 99%), hydrazine hydrate ($NH_2NH_2 \cdot H_2O$), sulfur, isopropanol were analytical grade. All reagents were used as received without further purification. De-ionized water was used in all experiments.

Preparation of water-soluble luminescent Ag_2S NCs

The aqueous S^{2-} source and Ag_2S NCs were prepared as previously reported with a slight modification.[33] 0.15 g of sulfur was dissolved in hydrazine hydrate (10 mL) and stirred at room temperature till sulfur was completely dissolved. The resultant transparent solution was deposited for 2 h at room temperature and diluted for 35 times before further application. 77 mg of glutathione and 25 mg of silver nitrate were dissolved in de-ionized water (10 mL) and supramolecular hydrogel was formed. After 1.1 mL of aqueous S^{2-} source was added, yellow transparent solution was obtained. The mixture was further stirred for 30 mins in the cool water. The obtained Ag_2S NCs were purified upon addition of isopropanol, centrifuged at 10,000 rpm to remove solvents and redispersed in de-ionized water for further application.

Application as Cu(II) probe

Stock solution of $CuSO_4$ with the concentration of 3 $mmol \cdot L^{-1}$ was prepared and various Cu^{2+} concentrations were diluted by serial dilution. To check the sensitivity of the NCs, other ions including Na^+, K^+, Ba^{2+}, Ca^{2+}, Cd^{2+}, Co^{2+}, Fe^{2+}, Fe^{3+}, Hg^{2+}, Mg^{2+}, Mn^{2+}, Zn^{2+}, Pb^{2+} were carried out. All the experiments were similar as performing for the detection of copper(II) ion.

Cellular Imaging

MC3T3-EI cells were cultured in high-glucose Dulbecco's modified Eagle's medium (DMEM) media supplemented with 10% fetal bovine serum (FBS) and 1% penicillin/streptomycin at 37°C using a humidified 5% CO_2 incubator. Suspensions (30 μg/mL) of Ag_2S NCs from the stock solution were prepared with serum-containing DMEM. MC3T3–E1 cells were seeded in six-well plates with a destiny of 1.5×10^5 cells/well for uptake experiments. The growth medium was replaced with the Ag_2S NCs suspensions 24 h after seeding, and incubation was for another 24 h at 37 ° C. Prior to fixation of the cells for inspection with a confocal fluorescence microscope, the excess Ag_2S NCs were removed by washing 3 times with warm phosphate buffered saline (PBS).

Characterization methods

UV/Vis absorbance spectra were recorded on a Cary 50 scan spectrophotometer at room temperature. The fluorescence spectra were recorded by using a Shimadzu RF-5301 spectrofluorimeter. TEM imaging was obtained with a JEM-2100F transmission electron microscope (TEM) operating at 200 kV. X-ray photoelectron spectroscopy (XPS) was obtained in a VG ESCALAB MKII spectrometer using Mg K_α excitation (1253.6 eV) and binding energy calibration was based on C 1s at 284.6 eV. The fourier transform infrared spectroscopy (FT-IR) was measured at wavenumbers ranging from 500 cm^{-1} to 4000 cm^{-1} using a Nicolet Avatar 360 FT-IR spectrophotometer.

Result and discussion

Synthesis of luminescent Ag_2S nanoclusters

Glutathione-directed (GSH) synthetic route of stable, water-soluble and luminescent Ag_2S nanoclusters is shown in Scheme 1. GSH and $AgNO_3$ were firstly dissolved in water and supramolecular hydrogel was formed due to the interaction between silver ion and GSH, which is similar to the previous literatures.[34] After that, the sulfur source ($S\text{-}NH_2NH_2 \cdot H_2O$) was added, the supramolecular gel disappeared and light yellow solution was obtained. Subsequently, the solution was stirred further for about 30 mins in the cool water. The obtained nanoclusters were purified by precipitating upon addition of isopropanol and redispersed in aqueous solution. Herein GSH is the key for the formation of stable nanoclusters. In the absence of GSH, silver ion and sulfur source could rapidly form large nanoparticles rather than stable and small nanoclusters. In addition, mild sulfur source also plays an important role in preparing fluorescent nanoclusters. According to the results of the experiments, other sulfur source such as Na_2S could not form stable and small fluorescent nanoclusters.

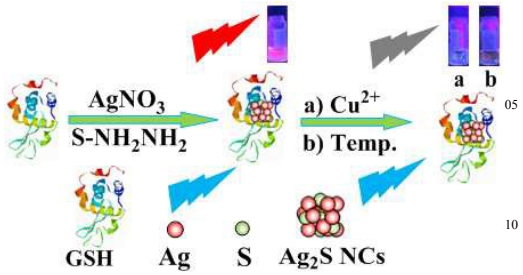

Scheme 1. Schematic illustration of the formation of Ag_2S nanoclusters (NCs) and Cu^{2+} ion together with higher temperatures (45°C) induced luminescent quenching of the NCs.

Cite this: DOI: 10.1039/c0xx00000x

www.rsc.org/xxxxxx

ARTICLE TYPE

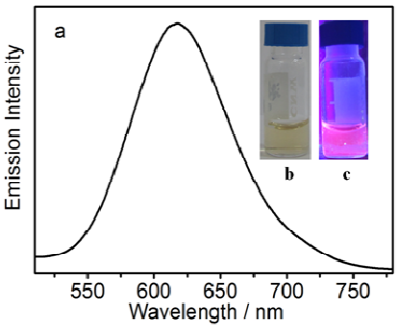

Figure 1. a) The fluorescent spectrum of Ag_2S NCs in aqueous solution. The inset images show the photographs of NCs (b) at the room temperature and (c) under a UV light with an excitation wavelength at 365 nm.

By adjusting the molar ratios of GSH and $AgNO_3$ at 3:1, intense red fluorescent Ag_2S nanoclusters with peak maximum at about 620 nm are obtained (Figure 1). The fluorescent quantum yields of clusters reach up to 1.9% using Rodamine 6G as standard. Other molar ratios of GSH and $AgNO_3$ (such as 2:1, 4:1, 5:1) will decrease the fluorescent quantum yields. In addition, freeze-dried Ag_2S powder also show strong red fluorescence under UV light (Figure S1). Furthermore, the newly synthesized nanoclusters show good water-soluble and no precipitation is observed, which is attributed to stabilizing effects of GSH to prevent large nanoparticles formed. Moreover, the obtained nanoclusters could give a well-defined excitation spectrum (Figure S2).

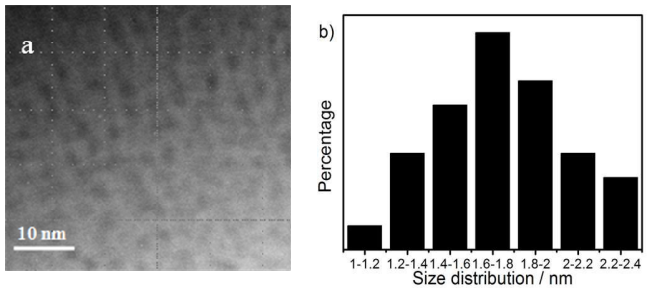

Figure 2. a) Typical TEM image of as-prepared Ag_2S NCs; b) Size distribution: the average size was 1.78 ± 0.3 nm.

The transmission electron microscope (TEM) image of Ag_2S NCs is shown in Figure 2. As indicated, the uniform NCs are spherical and dispersible with an average size of ~1.78 nm. Furthermore, there is no large particles and precipitation observed, which suggests the key template role of GSH for preventing the NCs from agglomerating. To further characterize the as-prepared Ag_2S NCs, X-ray photoelectron spectroscopy (XPS) is performed to determine chemical composition and chemical status of NCs. The XPS results of NCs are shown in Figure 3. The binding energy of Ag 3d appears at 367.9 eV rather than at 368.2 eV, which suggests that silver ions are univalent in nanoclusters.[35] The binding energy of S 2p is observed at 161.8 eV and 163.1 eV, which is in agreement with Ag–S and S. The peaks at 288.2, 285.8, and 284.6 eV are characteristic signals of C 1s, which is assigned as –C=O, –CH–, and $–CH_2CH_3$, respectively.[36] The binding energy of N 1s appears at 401.1 and 399.6 eV, which is assigned to $–NH_3^+$ and –NH–.[37] In addition, the surface chemistry is characterized by FT-IR (Figure S3). Comparing with the FT-IR spectra of Ag_2S NCs and pure GSH, it is obvious that the characteristic band at 2526 cm^{-1} of free thiol is absent for Ag_2S NCs, which suggests the formation of metal-S complexes. The results of fluorescence, photoluminescence excitation, transmission electron microscopy, X-ray photoelectron spectroscopy, and FI-IR spectra confirm that Ag_2S nanoclusters are successfully synthesized.

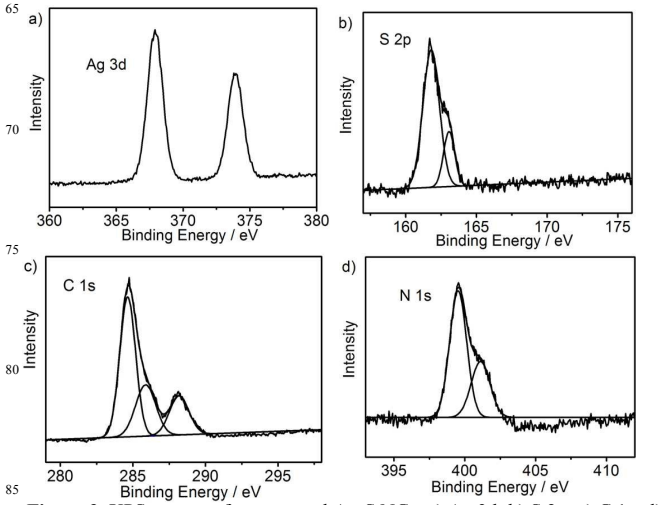

Figure 3. XPS spectra of as-prepared Ag_2S NCs: a) Ag 3d; b) S 2p; c) C 1s; d) N 1s.

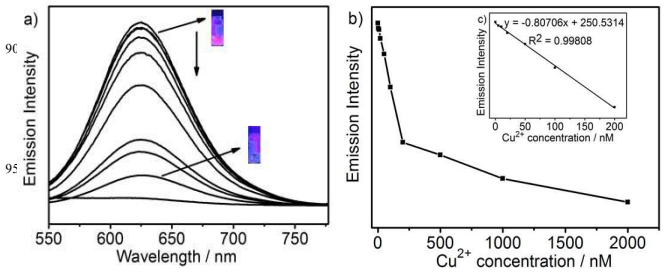

Figure 4. a) Emission spectral changes of Ag_2S NCs in water upon addition of different amounts of Cu^{2+} ions (0, 5, 10, 20, 50, 100, 200, 500, 1000, 2000 nM); b) Maximum emission intensity changes of a) as the function of different amounts of Cu^{2+} ions; c) Linear region of calibration curve (0–200 nmol·L^{-1} of Cu^{2+} ions).

Optical responses of luminescent Ag_2S nanoclusters to Cu^{2+} ion

As a natural biomolecule, GSH has several functional groups including amino and carboxyl groups which encourages the samples to have good dispersion in aqueous solution. Especially, GSH has a much-stronger affinity towards metal ions, such as Cu^{2+}, Pb^{2+}, Hg^{2+}, which has great potential as probe for ion detection. Upon addition of different amounts of Cu^{2+} ions into the aqueous solution of Ag_2S nanoclusters, the results show that the luminescence of Ag_2S NCs is gradually quenched with the increasing of the concentration of Cu^{2+} ion. The emission spectral

changes of NCs upon addition of different amounts of Cu^{2+} ion is shown in Figure 4. Furthermore, a linear proportionality between luminescent intensity and the concentration of Cu^{2+} ions is observed over the range from 0 nmol·L^{-1} to 200 nmol·L^{-1}, which is also shown in Figure 4. Moreover, the limit of detection is estimated to be 2.5 nmol·L^{-1} in terms of a signal-to-noise of 3.

To test the sensitivity and selectivity of fluorescent quenching by Cu^{2+} ion, other metal ions, such as Na^{+}, K^{+}, Ba^{2+}, Ca^{2+}, Cd^{2+}, Co^{2+}, Fe^{2+}, Fe^{3+}, Hg^{2+}, Mg^{2+}, Mn^{2+}, Zn^{2+}, Pb^{2+}, Hg^{2+}, are also applied for the specificity study of the fluorescent probe. These ions are performed under the same conditions as Cu^{2+} ion. The responses of the nanoclusters over these ions manifested by the emission intensity variation are displayed in Figure 5. The results clearly show fewer emission intensity changes are observed for other ions relative to Cu^{2+} ion, which demonstrates that our material is highly sensitive and selective for Cu^{2+} ion.

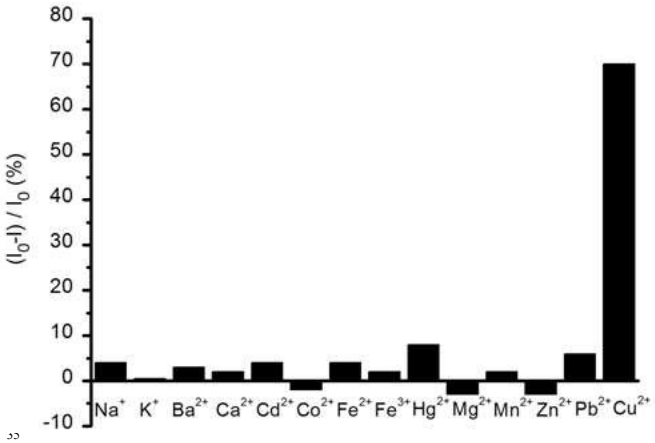

Figure 5. Relative emission intensity $(I_0–I)/I_0$ of as-prepared Ag_2S NCs upon addition of 10^{-6} mol·L^{-1} of different metal ions. I_0 and I represent the maximum emission intensity of Ag_2S NCs before and after addition of metal ions.

The reasons for highly selective fluorescent probe for Cu^{2+} ion is due to aggregation-induced fluorescent quenching of NCs, which has been reported in the previous paper.[38] In fact, the surface of NCs protected by GSH is crucial for highly selective for Cu^{2+} ion mainly induced by the complexation aggregation between NCs and Cu^{2+} ions. The complexation aggregation of NCs with Cu^{2+} ions is also confirmed by TEM images shown in Figure S4. The results suggests that Cu^{2+} ion induced the formation of larger nanoclusters with the size at about 3.16 ± 0.4 nm, which causes the luminescent quenching of NCs and has been widely used as probes to measure metal ions.[39]

Table 1. Recoveries of copper ions spiked in tap water, mineral water, and Taihu lake water by the Ag_2S nanocluster probe.

	tap water			mineral water		
added Cu^{2+} (nM)	found Cu^{2+} (nM)	Recovery (%)	RSD (%)	found Cu^{2+} (nM)	Recovery (%)	RSD (%)
9.9	10.7	108.0	8.7	10.8	109.1	6.3
14.8	15.1	102.1	6.5	15.3	103.4	7.9
19.7	19.6	99.5	3.9	20.8	105.6	3.2
	Taihu lake water					
added Cu^{2+} (nM)	found Cu^{2+} (nM)	Recovery (%)	RSD (%)			
9.9	9.5	95.9	6.7			
14.8	15.1	102.1	3.6			
19.7	20.6	104.6	2.8			

To further assess its applications in real water samples, the Ag_2S nanoclusters were applied to detect Cu^{2+} ion including tap water, mineral water, and Taihu lake water with different amounts of Cu^{2+} ion. Real water samples are first filtered to remove any solid suspension. Studies are performed with ten concentrations (0, 5, 10, 15, 20, 25, 30, 200, 500, 1000 nmol·L^{-1}) in each real water. It is clear that fluorescent intensity gradually decreases with the increase of the concentration of Cu^{2+} ion and a linear relationship between fluorescent intensity of NCs and the concentration of Cu^{2+} ion is observed over the range from 0 to 25 nmol·L^{-1} (Figure S5–S7). These results indicate that such a sensor system is highly sensitive towards Cu^{2+} ion in real water samples. Furthermore, the recovery tests (Table 1) are performed in the three types of water samples with a fixed amount of Cu^{2+} ion (9.9, 14.8, 19.7 nmol·L^{-1}), and the relative standard deviations of the water samples are close to 100% (from 95% to 110%), which suggests that the fluorescent method performs well for Cu^{2+} ion detection in real water.

Optical responses of luminescent Ag_2S nanoclusters to temperature

With the increase of the temperature from 6°C to 50°C, the fluorescent intensity of Ag_2S nanoclusters is greatly quenched more than 97% and emission maximum peak do not show shift within the investigated temperature window. The temperature dependence of the emission intensity is shown in Figure 6. A careful investigation on the variation between the fluorescent intensity and temperature is performed. A linear relationship between the logarithm of fluorescent intensity and temperature ranging from 6°C to 50°C is observed. In view of the temperature range larger than physiological temperature, the temperature probe have promising applications in cell and in vivo temperature sensing.[9] Furthermore, the temperature response of the probe is reversible upon temperature cycles and a slight temperature hysteresis during heating and cooling processes is observed between 15°C and 40°C for five temperature cycles (Figure S8).

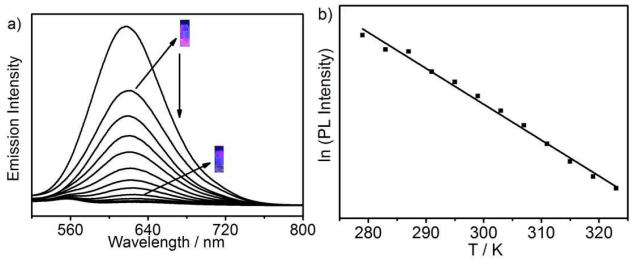

Figure 6. a) Emission spectral changes upon increasing the temperatures from 279 K to 323 K; b) Linear relationship between the logarithm of emission intensity and temperatures.

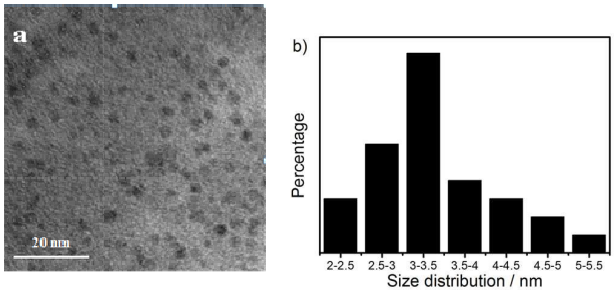

Figure 7. a) The TEM image of Ag_2S NCs in aqueous solution at 318 K; b) Size distribution: the average size was 3.46 ± 0.5 nm.

Cite this: DOI: 10.1039/c0xx00000x

www.rsc.org/xxxxxx

ARTICLE TYPE

To further understand fluorescent quenching mechanism over temperature changes, TEM is used to study temperature-responsive behavior of nanoclusters. As illustrated in Figure 7, the average diameters of nanoclusters is about 3.46 nm at 45°C. As contrast, the average diameter of NCs at room temperature is about 1.78 nm. Hence, with the increasing of the temperature, the aggregation of Ag_2S nanoclusters induce the obvious fluorescent quenching.

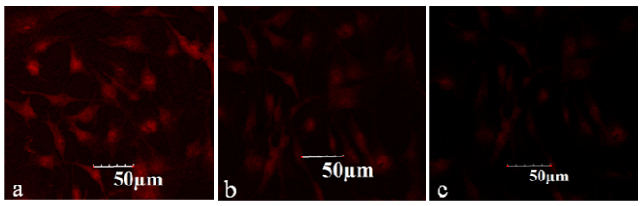

Figure 8. Confocal fluorescent images of MC3T3-EI cells incubated with Ag_2S naoclusters for 24 h measured at about (a) 20°C; (b) 30°C; (c) 40°C.

To deeply understand nanothermometry devices for temperature sensing in cell, the MC3T3-EI cellular imaging of Ag_2S nanoclusters at 20°C, 30°C, 40°C was evaluated by confocal fluorescence microscopy. Figure 8 revealed that the confocal fluorescence images of MC3T3-EI cells incubated with Ag_2S nanoclusters at the concentration of 30 μg/mL for 24 h, whose fluorescence was in the NIR region. From the fluorescence images of the MC3T3-EI cells, we can see the cells incubated with Ag_2S nanoclusters maintain their normal morphology, suggesting the good biocompatibility at this dose and time point. The fluorescence images irradiated by 515 nm show red fluorescence within the cells and the fluorescence signal was not only distributed in the cytoplasm but also in the cellular nucleus. In addition, the fluorescence image was greatly quenched with the increase of the temperature. The results indicate that the as-prepared NCs could be used as versatile nanothermometry devices in cellular temperature sensing based on obvious temperature dependence on the logarithm of fluorescence emission intensity.

Conclusion

In summary, we have developed a new dual fluorescent sensors for detection of copper ion and temperature based on glutathione protected Ag_2S nanoclusters by a one-step method. As-prepared NCs showed red fluorescence with peak maximum at about 620 nm and quantum yields up to 1.9%. Owing to the surface protection of glutathione, which has good dispersion in aqueous water and strong affinity toward metal ions, the NCs exhibit significant copper(II)-tfluorescence quenching mechanism with a detection limit of 2.5 nmol·L^{-1}, which suggests that the novel Ag_2S NCs have great potential for detection of copper(II) in the environmental samples. In addition, the temperature dependence on the logarithm of the fluorescence emission intensity attributing to aggregation-induced fluorescence quenching mechanism has also been observed and approximately linear in physiological temperature range, which makes the NCs promising candidate in cellular and in vivo temperature sensing. This work may provide an alternative way to develop multifunctional nanoclusters as a probe for metal ions and temperature, and expand the applications of glutathione protected silver nanoclusters.

Acknowledgements

This work was supported by the Health Bureau Foundation of Wuxi City, China (MS201524). We also acknowledge support from Wuxi Center for Disease Control and Prevention, China.

Notes and references

[a]*Wuxi Center for Disease Control and Prevention, Wuxi 214023, P.R. China; E-mail: konglingcan2010@163.com; wxcdclingxia@sina.com*

[b]*Department of Basic Science, Jilin Jianzhu University, Changchun 130118, P. R. China;*

† Electronic Supplementary Information (ESI) available: [details of any supplementary information available should be included here]. See DOI: 10.1039/b000000x/

1. A. Das, S. Bhattacharya, M. Palaniswamy and J. Angayarkanni, *World J. Microbiol. Biotechnol.*, 2014, **30**, 2315–2324.
2. S. Borowska and M. M. Brzóska, *J. Appl. Toxicol.*, 2015, **35**, 551–572.
3. S. P. Ng, E. A. Palomb and M. Bhave, *World J. Microbiol. Biotechnol.*, 2012, **28**, 2221–2228.
4. N. Quiroz, N. Rivas, T. D. Pozo, J. Burkhead, M. Suazo, M. González and M. Latorre, *Biometals*, 2015, **28**, 321–328.
5. R. Dobrowolski, A. Mróz, M. Otto and M. Kuryło, *Microchem. J.*, 2015, **121**, 18–24.
6. Y. Makonnen and D. Beauchemin, *Spectrochim. Acta B*, 2014, **99**, 87–93.
7. M. L. Lin and S. J. Jiang, *Food Chem.*, 2013, **141**, 2158–2162.
8. L. Kong, H. L. Wong, A. Y. Y. Tam, W. H. Lam, L. Wu and V. W. W. Yam, *ACS Appl. Mater. Interfaces*, 2014, **6**, 1550−1562.
9. G. Kucsko, P. C. Maurer, N. Y. Yao, M. Kubo, H. J. Noh, P. K. Lo, H. Park and M. D. Lukin, *Nature*, 2013, **500**, 54–58.
10. K. Okabe, N. Inada, C. Gota, Y. Harada, T. Funatsu and S. Uchiyama, *Nat. Commun.*, 2012, **3**, 705–713.
11. F. Vetrone, R. Naccache, A. Zamarrón, A. J. Fuente, F. Sanz-Rodríguez, L. M. Maestro, E. M. Rodriguez, D. Jaque, J. GarcíaSolé and J. A. Capobianco, *ACS Nano*, 2010, **4**, 3254–3258.
12. P. Yu, X. Wen, Y. R. Toh and J. Tang, *J. Phys. Chem. C*, 2012, **116**, 25552–25557.
13. E. S. Shibu, K. Ono, S. Sugino, A. Nishioka, A. Yasuda, Y. Shigeri, S. Wakida, M. Sawada and V. Biju, *ACS Nano*, 2013, **7**, 9851–9859.
14. G. Kwak, S. Fukao, M. Fujiki, T. Sakaguchi and T. Masuda, *Chem. Mater.*, 2006, **18**, 2081–2085.
15. Y. Hiruta, M. Shimamura, M. Matsuura, Y. Maekawa, T. Funatsu, Y. Suzuki, E. Ayano, T. Okano and H. Kanazawa, *ACS Macro Lett.*, 2014, **3**, 281–285.
16. S. A. Claridge, A. W. Castleman, J. S. N. Khanna, C. B. Murray, A. Sen and P. S. Weiss, *ACS Nano*, 2009, **3**, 244–255.
17. K. Judai, S. Abbet, A. S. Wörz, U. Heiz and C. R. Henry, *J. Am. Chem. Soc.*, 2004, **126**, 2732–2737.
18. A. George, E. S. Shibu, S. M. Maliyekkal, M. S. Bootharaju and T. Pradeep, *ACS Appl. Mater. Interfaces*, 2012, **4**, 639–644.
19. R. R. Holmes, *Acc Chem. Res.*, 1989, **22**, 190–197.
20. C. Wang, L. Xu, X. Xu, H. Cheng, H. Sun, Q. Lin and C. Zhang, *J. Colloid Interf. Sci.*, 2014, 416, 274–279.
21. L. Zhang and E. Wang, *Nano Today*, 2014, **9**, 132—157.
22. C. Wang, L. Xu, Y. Wang, D. Zhang, X. Shi, F. Dong, K. Yu, Q. Lin and B. Yang, *Chem. Asian J.*, 2012, **7**, 1652–1656.
23. L. Zhang, J. Zhu, J. Ai, Z. Zhou, X. Jia and E. Wang, *Biosens. Bioelectron.*, 2013, **39**, 268–273.
24. J. Zhang, L. Tu, S. Zhao, G. Liu, Y. Wang, Y. Wang and Z. Yue, *Biosens. Bioelectron.*, 2015, **67**, 296–302.

25. C. Wang, Z. Xu, H. Cheng, H. Lin, M. G. Humphrey and C. Zhang, *Carbon*, 2015, **82**, 87–95.
26. L. Zhang and E. Wang, *Nano Today*, 2014, **9**, 132–157.
27. W. Chen, X. Tu and X. Guo, *Chem. Commun.*, 2009, 1736–1738.
28. M. Santhosh, S. R. Chinnadayyala, A. Kakoti and P. Goswami, *Biosens. Bioelectron.*, 2014, **59**, 370–376.
29. X. Jiang, C. Sun, Y. Guo and G. Nie, L. Xu, *Biosens. Bioelectron.*, 2015, **64**, 165–170.
30. Y. Yue and X. Wang, Nano Rev., 2012, 3, 11586–DOI: 10.3402/nano.v3i0.11586.
31. Z. Wang, L. Si, J. Bao and Z. Dai, *Chem. Commun.*, 2015, **51**, 6305–6307.
32. A. L. Sun, F. C. Jia, Y. F. Zhang and X. N. Wang, *Microchim. Acta*, 2015, **182**, 1169–1175.
33. C. Wang, Y. Wang, L. Xu, D. Zhang, M. Liu, X. Li, H. Sun, Q. Lin and B. Yang, *Small*, 2012, **8**, 3137–3142.
34. Y. Jiang, X. Yang, C. Ma, C. Wang, H. Li, F. Dong, X. Zhai, K. Yu, Q. Lin and B. Yang, *Small*, 2010, **6**, 2673–2677.
35. J. Yang and J. Y. Ying, *Angew. Chem. Int. Ed.*, 2011, **50**, 4637–4643.
36. F. Xia, L. Feng, S. Wang, T. Sun, W. Song, W. Jiang and L. Jiang, *Adv. Mater.*, 2006, **18**, 432–436.
37. E. S. Shibu and T. Pradeep, *Chem. Mater.*, 2011, **23**, 989–999.
38. C. Wang, H. Cheng, Y. Sun, Z. Xu, H. Lin, Q. Lin and C. Zhang, *Microchim. Acta*, 2015, **182**, 695–701.
39. F. Wen, Y. Dong, L. Feng, S. Wang, S. Zhang and X. Zhang, *Anal. Chem.*, 2011, **83**, 193–1196.

Cite this: DOI: 10.1039/c0xx00000x

www.rsc.org/xxxxxx

ARTICLE TYPE

TOC

Highly red luminescent Ag_2S nanoclusters were synthesized and they show higher sensitivity as nanosensors for copper(II) ion and temperature.